GPS CONSTRAINTS ON GARLOCK AND EASTERN CALIFORNIA SHEAR ZONE

FAULT SLIP RATES

By

CHRISTINA KING

A Thesis Submitted to The Honors College

In Partial Fulfillment of the Bachelor's degree
With Honors in

Geophysics

THE UNIVERSITY OF ARIZONA

May 2009

Approved by:

Richard A. Bennett
Geosciences

## STATEMENT BY AUTHOR

I hereby grant to the University of Arizona Library the nonexclusive worldwide right to reproduce and distribute my thesis and abstract (herein, the "licensed materials"), in whole or in part, in any and all media of distribution and in any format in existence now or developed in the future. I represent and warrant to the University of Arizona that the licensed materials are my original work, that I am the sole owner of all rights in and to the licensed materials, and that none of the licensed materials infringe or violate the rights of others. I further represent that I have obtained all necessary rights to permit the University of Arizona Library to reproduce and distribute any nonpublic third party software necessary to access, display, run, or print my thesis. I acknowledge that University of Arizona Library may elect not to distribute my thesis in digital format if, in its reasonable judgment, it believes all such rights have not been secured.

SIGNED: _____

# GPS CONSTRAINTS ON GARLOCK AND EASTERN CALIFORNIA SHEAR ZONE FAULT SLIP RATES

Christina King[1] and Richard A. Bennett[1]

[1]*Department of Geosciences, University of Arizona*

**Abstract**. Previous geodetic studies of the Garlock fault of Southern California have found left lateral slip rates that are below geologic rate estimates. Our study develops a model for crustal deformation based on Quaternary faults of the southwest United States, and Global Positioning System (GPS) velocities. We used velocity estimates from the SCEC Crustal Motion Map, v. 3, the PBO, PBO NUCLEUS, SCIGN, and BARGEN continuous GPS networks to constrain this model. Using a simplified crustal deformation model we estimate relative block motions to match observational crustal velocities. The blocks are assumed to be elastic, deforming along their edges to simulate interseismic strain accumulation on active faults. The eastern Californian shear zone was divided into 8 blocks separated by 22 fault segments. Dividing the Garlock fault into five segments allowed for variation in slip rate along the fault system. We tested several model scenarios, under different assumptions about block rotation. For our preferred model, we estimate rates of $2.96 \pm 0.15$, $2.81 \pm 0.15$, $3.04 \pm 0.16$, and $2.79 \pm 0.15$ mm/yr of left lateral slip starting along the western Garlock and moving east. On the east most segment, we found a rate of $0.82 \pm 0.09$ mm/yr, right lateral. Slip rates are fairly consistent to the west with a large drop in amplitude along the east most segment of the Garlock fault. Despite the consistency of the western segments, these rates are significantly lower than geologic rates of $7 \pm 2.5$ mm/yr. The discrepancy of rates along with the right lateral motion along the eastern segment may suggest a complex role of the Garlock fault in the Eastern California Shear zone. The difference between the geological rates and geodetic rates may imply the importance that a time scale has on fault rates, but it could also indicate biases in either the geodetic or geologic estimates. The importance of the Garlock fault discrepancy derives from the fact that the "missing motion" explanation for geodetic-geologic discrepancy requires that the geodetic rates be higher. Thus, the discrepancy may result from transient postseismic deformation biasing the geodetic rate estimate downward, or it may represent a real discrepancy in slip rate.

## Introduction

The eastern California shear zone (ECSZ) lies between the North American and Pacific plates and east of the San Andreas fault. The San Andreas fault accommodates 70% of the total motion between these two plates (Meade and Hager 2005). Other fault zones such as the ESCZ accommodate the rest of slip and this slip rate decreases from the Pacific plate to the North

American plate. A slip rate of 11.3 ± 0.3 mm/yr across the ECSZ is calculated from the motion

of Serria Nevada and Eastern Basin and Range poles (McCaffrey 2005). Faults trending parallel

to plate motion have a right-lateral motion and the faults trending perpendicular to plate motion

have a left lateral motion such as the Garlock (McGill 2003). Previous geodetic studies have

found that there have been discrepancies between geologic and geodetic slip rate estimates.

Many have theorized that geodetic estimates may be higher or lower that geologic estimates due

to the influence of the transient postseismic phase of the earthquake cycle, but not all

discrepancies follow large earthquakes (e.g., Oskin et. al 2008). Another explanation for the

geodetic-geologic discrepancy would argue that geologic methods, which focus on specific
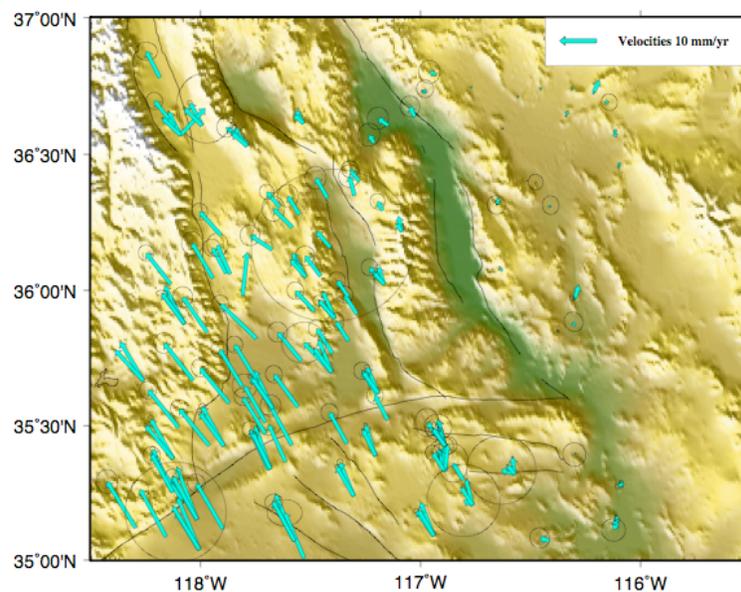


Figure 1: Our block model area with observational in blue and active faults the thin black lines. Vectors point in the direction the station is moving and error of the measurements are drawn in circles around the head of the arrows.

strands of complex fault zones do not characterize all of the motion accommodated across the zone.  According to this hypothesis, geodetic methods sense the total motion including the "missing motion" that is not visible to geology.  However, our study of the Garlock fault shows that geodetic rates are lower than geologic rates but postseismic influence may still be factor. Studying the discrepancy between geologic and geodetic could provide better understanding of fault mechanics and earthquake prediction.

**Geologic Positioning System Data**

The set of GPS stations that we used comprise a collection of continuous networks, specifically the PBO NUCLEUS, SCIGN, and BARGEN networks and velocities for the SCEC Crustal Motion Map v.3**.**  We excluded COSO, part of the SCIGN network, in this study because it in the vicinity of a geothermal field and as a result its motions are not linear through time. The COSO area is sometimes modeled as its own micro-plate due to its unusual movement (Frankel et al. 2009).

**Method**

**Block Modeling**

The deformation between two blocks can be modeled in different ways. We estimate the motion between the North America and Pacific plate to be accommodated by rotating elastic blocks that slip past one another analogous to the motions of the larger tectonic plates.  Similar to the tectonic plates, we assume that the blocks in our model have minimal internal deformation. This assumption is supported by geologic surveys of the deformation in area (Garfunkel 1974). This allows for the strain to accumulate along the faults that separate the blocks and provides

insight to the role of the Garlock fault.  The block boundaries represent finite length vertical fault

segments but in actuality the faults in this area may dip at some depth and are not always

connected (McCaffrey 2005). Our model includes the area from 34.98N to 36.80 N and 118.3W

to -116W that is split into 8 blocks divided into 22 fault segments.  The block modeling method

is described in detail by Spinler et al. (in prep).   Slip rates are calculated using the relative

motions of the blocks surrounding the fault.  We used this method invert GPS velocities for fault



Figure 2: Our block model is displayed in bold black lines and the residual velocity of our block
model in blue.  The difference between the model velocities and the observed velocities were
plotted as residuals. Abbreviations for the faults are placed on the figure.

slip (strike and tensile components) and vertical axis rotation rate. Residual velocities to the best

fitting model have a mean value of 1.3 mm/yr.  The normalized RMS (NRMS) was found to be

2.01 and the residuals are less than the normalized RMS. However, the NRMS is not close to 1

and for this reason we inflated the error of the study by the NRMS.

The block geometry that we used is shown in Figure 2. Fault locking depths were set to 15 km. The Sierra Nevada (SN), Owens Valley (OV), Eastern Mojave (EM), Calico Blackwater (CB) and the Mojave (M) blocks were allowed to rotate, but rotation rates for all other blocks in the model were fixed to zero. Rotation of the blocks necessitates slip rate variation along strike for faults bounding the rotating blocks (McCaffrey 2005). We tested a model wherein none of the blocks were allowed to rotate. For this test model, we concluded that the strike slip rates became unreasonable on some of the faults especially the Mojave Desert faults. We also tested a model wherein the SN, OV, CB and M blocks were allowed to rotate and the EM block was not allowed to rotate. This test model had similarly unreasonable fault slip rates. Thus our preferred model includes the rotation of these blocks. Locking depth models of the San Andreas and other geodetic studies done in the ECSZ support our choice of locking depth (Chery 2008; McClusky et al. 2001; Savage and Burford 1973). It may not be unreasonable that locking depths of the ECSZ could be modeled around similar locking depths as elastic thicknesses as the San Andreas, because of their similar lithospheric properties. Garfunkel (1974) and Oskin and Iriondo (2004) support rotation of blocks in this area especially of the blocks of the Mojave Desert. With the model constrained with a locking depth of 15 km and rotating of specific blocks especially the blocks south of the Garlock residuals are found using a best fit to the data.

**Strain**

We used the GPS velocity field to estimate the strain rate field to compare to the strike and tensile rates observed in our block model. We used the code SSPx (Cardozo and Allmendinger, 2008) to estimate the strain rate field using a least squares inversion of observational GPS velocities. Velocities were weighted by distance from the stations to a calculated strain rates at a point of interest. This method allowed calculation of maximum shear,

dilatational, rotational, extensional and compressional strain. Displayed in this study are the maximum shear strain and dilatational strain.

## Discussion

### Block Modeling

Through the use of block modeling we found that a locking depth on all the faults to be 15 km, the rotation of the SN, OV, PV, EM, CB and the M blocks and the COSO site elimination created the best fit residuals. No residual was greater than 4.1 mm/yr. The average residual was 1.3 mm/yr. However, the residuals were heavily weighted to a much lower magnitude. The NRMS was found to be 2.01, which constrains our residuals fairly well. The error of the strike and tensile rates were weighted with the NRMS to account for possible underestimate of the error.

Our estimates for the strike-slip and tensile slip rates are listed in Table 1 with their uncertainties. In the northern ECSZ, we found right lateral strike slip rates, increasing from $2.95 \pm 0.08$ mm/yr along the Fish Lake (FL)/ Death Valley (DV) system to $4.06 \pm 0.10$ mm/yr along the Panamint Valley (PV) system to $5.30 \pm 0.14$ mm/yr along the Owens Valley (SN/AL) system. Other geodetic surveys have found the PV system to be closer in magnitude to the FL/DV system but consistent with the SN/AL system having the highest strike rate (McClusky et al. 2001). The SN and AL faults have geologically determined slip rates lower than our geodetic estimates at $2.6 \pm 0.5$ mm/yr (McCaffrey 2005; Dixon et al. 2003). This discrepancy could be caused by the earthquake cycle or strain partitioning in this area (Dixon et al. 2003).

South of the Garlock fault, the ECSZ is more complex and does not display uniform slip rates across the Mojave Desert. Along the Blackwater (BW) fault, a right lateral slip rate of 3.42

| Fault Name | Abbreviation | Strike Rate (mm/yr) | Tensile Rate (mm/yr) |
|---|---|---|---|
| Airport Lake | AL | $5.03 \pm 0.13$ | $-1.76 \pm 0.08$ |
| Black Mountain | BMa | $3.01 \pm 0.08$ | $0.33 \pm 0.05$ |
| Black Mountain | BMb | $2.88 \pm 0.08$ | $-0.92 \pm 0.05$ |
| Black Water | BWa | $3.42 \pm 0.21$ | $2.03 \pm 0.09$ |
| Goldstone | GSa | $1.68 \pm 0.21$ | $-12.64 \pm 0.39$ |
| Goldstone | GSb | $-0.10 \pm 0.45$ | $-7.35 \pm 0.21$ |
| Tiefort | TF | $-8.53 \pm 0.17$ | $-1.75 \pm 0.21$ |
| West most Garlock | G | $-2.96 \pm 0.15$ | $3.50 \pm 0.12$ |
| West Garlock | Ga | $-2.81 \pm 0.15$ | $-0.38 \pm 0.07$ |
| West Central Garlock | Gb | $-3.04 \pm 0.16$ | $2.02 \pm 0.16$ |
| East Central Garlock | Gc | $-2.80 \pm 0.15$ | $0.79 \pm 0.13$ |
| East Garlock f | Gd | $0.82 \pm 0.09$ | $4.05 \pm 0.09$ |
| Hunter Mountain | HMa | $4.22 \pm 0.11$ | $-0.69 \pm 0.19$ |
| Hunter Mountain | HMb | $3.85 \pm 0.14$ | $1.92 \pm 0.14$ |
| Extension of Death Valley | MUc | $3.57 \pm 0.08$ | $0.45 \pm 0.06$ |
| North Fish Lake Valley | NFLV | $2.99 \pm 0.08$ | $0.38 \pm 0.05$ |
| North Panamint Valley | Pva | $4.06 \pm 0.14$ | $-0.68 \pm 0.08$ |
| Panamint Valley | PVb | $3.82 \pm 0.14$ | $-1.61 \pm 0.07$ |
| South Panamint Valley | PVc | $4.47 \pm 0.10$ | $0.25 \pm 0.15$ |
| Southern Death Valley | SDV | $2.95 \pm 0.08$ | $0.65 \pm 0.05$ |
| Southern Sierra Nevada | SSNb | $5.28 \pm 0.14$ | $-1.77 \pm 0.25$ |
| Southern Sierra Nevada | SSNc | $5.32 \pm 0.14$ | $-0.54 \pm 0.14$ |

Table 1: Displays the fault name and abbreviations. Negative values for strike rate indicate left-lateral motion. Negative values for tensile rate indicate extension along the faults.

$\pm 0.21$ mm/yr is observed. Along the northern Goldstone (GS) there is $1.68 \pm 0.21$ mm/yr and the southern GS it was found that the slip rate would be left lateral $0.10 \pm 0.45$ mm/yr. The southern GS fault may also be right lateral as the uncertainties are large here. These two fault systems, the BW and GS zones, have geologically been found to right lateral fault zones. Specifically, geologic studies based on geochronology and geologic mapping have indicated that there is a long-term slip rate across the BW fault of $0.49 \pm 0.04$ mm/yr (Oskin and Iriondo 2004; Oskin et al. 2007). The discrepancy between the geologic rate and our rate is purposed to be a non-steady and fluctuating strain along the BW fault (Oskin and Iriondo 2004). The Tiefort (TF) fault has a

left lateral slip rate of 8.53 ± 0.17 mm/yr. This is a large estimate as compared to any other

geologic rates for the Mojave Desert, which have been determined to be no greater than 1 mm/yr

(Oskin et al. 2007). There is an inconsistency in previous studies as to whether a fault, located

where the TF fault is located, is included in the block models (Frankel et al. 2008; Oskin et al.

2007; Schermer et al. 2001).  The omission of the fault may indicate that these studies believe it

to be inactive or have a negligible slip. However, in our study including this fault reduced the

residuals substantially. Due to the nature of our data set, the velocities in this area consist of both

continuous and campaign stations. There are three possibilities for this anomalously large rate.

One is that the GPS velocities could be having a biasing effect on the strike rates due to the large

error of the campaign sites. Two, it is possible that there is more diffuse deformation through the

interior of the block and third that the slip rate is taken up along the eastern most Garlock

segment is being modeled along this segment.

The Garlock fault was divided up into 5 segments and separates the northern ECSZ from

the northern Mojave Desert. From the west end, we estimate left lateral slip rates of 2.96 ± 0.15,

2.81 ± 0.15, 3.04 ± 0.16, 2.80 ± 0.15 mm/yr and along the eastern portion was found to be 0.82 ±

0.08 mm/yr right lateral strike slip. The geologic rates have ranged from 5-10 mm/yr along the

Garlock with a best estimate of 7.6 mm/yr along the west end (McGill et al. 2009).  However,

because most of the previous studies have taken place along the central and western end they

may not be sampling this eastern side of the fault. Other geodetic surveys have shown fault rates

ranging from 1 to 4 mm/yr of left lateral slip and eliminate the eastern portion all together

(McClusky et al. 2001). The elimination of this eastern end may imply that the slip has minimal

influence of their study, is not believed to be active, or there is not enough data in this area. Our

results for the eastern end of the Garlock could be biased because of the lack of GPS sites in this

area. Additional surveys in the eastern part of Garlock would determine if this rate anomaly is an artifact or correct.

Studies of earthquakes in the ECSZ suggest that geodetic studies do not eliminate the effects that the earthquake cycle and do not account for the viscoelastic behavior of the lithosphere (Malservisi et al. 2003). The large earthquakes that would possibly have an effect on geodetic surveys would be the 1872 Owens Valley, 1952 Kern County, 1992 Landers and 1999 Hector Mine earthquakes (Fay et. al 2008; Oskin 2008). The data set that we use includes observatiobsn from various periods of time following these earthquakes. Because uncertainties persist in our knowledge of the rheological structure of the crust and upper mantle, we do not yet confidently know how persistent postseismic effects are, nor how far reaching. it is possible that the postseismic deformation due to these earthquakes has limited effects on our block model because of the size of our model, which averages out the velocities of the sites.
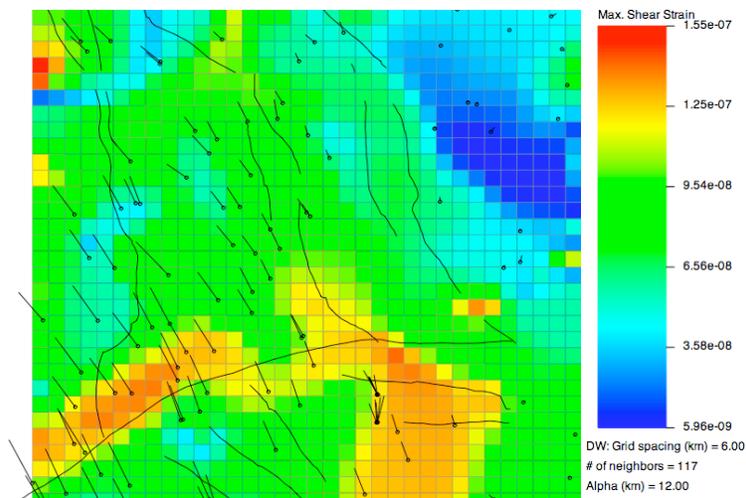


Figure 3: Maximum shear strain is displayed for our block model area. Active fault lines are drawn in a thin black line to give a reference point. GPS stations are drawn as open circles with their velocities drawn from the station in the direction the stations are moving in.

**Strain**

North of the Garlock fault, the maximum shear strain is fairly constant, with a low

maximum shear strain in the center of the northern blocks including the Sierra Nevada, Panamint Valley, Death Valley blocks and the North American plate. The fact that the strain across these faults does not peak like the strain across the Garlock and is fairly consistent across the three fault zones may supports evidence for a zone of shear strain that is not focused on one specific fault zone but is shared by all three fault zones.

The large peak of maximum shear strain around the GS and TF faults may help explain why there is not a constant slip velocity across all the faults in the southern ECSZ. The maximum strain does correlate with the maximum strike rate in this area of $8.53 \pm 0.17$ mm/yr along the Eastern Mojave. However, it does not correlate with high slip along the GS fault. The BW fault has similar magnitude of slip as the northern ECSZ and similar magnitude of shear strain. Strain calculated through geodetic methods across the Mojave Desert is generally twice as high as strain calculated through seismological, geologic mapping and geochronology (Oskin and Iriondo 2004; Frankel et al. 2008). Strain calculated through Synthetic Aperture Radar Interferometry (InSAR) has revealed that in the Mojave Desert region, right-lateral strain is more prevalent than left-lateral strain and that there is a large accumulation of shear strain along the BW fault (Peltzer et al. 2001). Our results do not show this peak of shear strain along the BW fault but rather along the TF fault but are consistent with higher geodetic rates than geologic slip rates.

The maximum shear strain calculated in our block model area is displayed in Figure 3. There is a peak along fault zones such as the Garlock and the TF faults as well as near the GS fault. The maximum shear strain along the Garlock peaks around the western end, appears to creep up the PV fault, and peaks along the DV fault. Along the Garlock there is an offset in the strain about where our Ga and Gb fault segments meet. This strain calculation may suggest a

partitioning of the northwest/southeast trending strain created by the movement of the Pacific

and North American plates.  Since there is a right lateral step in the strain it might be possible

that the BW/AL fault is cross cutting the Garlock and thus creating this side step in strain.

However, there is no geologic evidence of the northwest trending faults cross cutting the Garlock

(Frankel et al. 2008).  Previous geodetic studies have suggested that there is only a small amount

of left lateral strain accumulating along the Garlock relative to the large amount of right lateral

strain accumulating around it (McGill et al. 2009). The offset in our maximum shear strain data

may confirm that northwest-directed right lateral strain is dominating the east-northeast directed
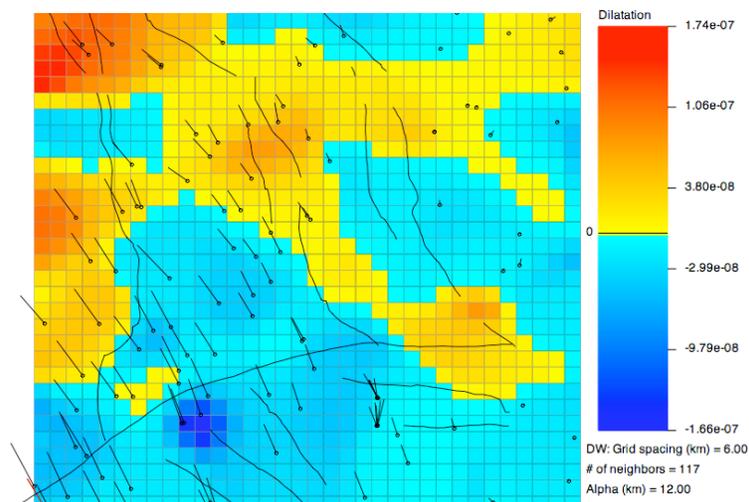
left lateral strain of the Garlock fault.



Figure 4: Displays dilatational strain. The thin black lines are the active faults in the ECSZ. The open circles are GPS sites and the strait lines protrude from the station in the direction the GPS site is traveling in.

Dilatation is calculated and displayed in Figure 4. There is maximum extension along the

north of the block model displaying peaks in the Sierra Nevada block, along the Panamint Valley

and along the eastern end of the Garlock fault. Therefore, extension is located between the major

right-lateral strike-slip faults of the ECSZ north of the Garlock (McGill et al. 2009; Frankel et. al

2008). The compression is significant where the Garlock and BW fault intersect.   Compression

along the central portion of the Garlock and extension along the eastern end of the fault supports clockwise rotation of the Mojave Desert (Schermer et al. 2001; McClusky et al. 2001).

**Conclusion**

The faults trending northwest are right lateral by our calculations and have higher geodetic rates than the geologic rates calculated for these faults. The faults trending east-northeast, at high angle to North American-Pacific relative plate motion are all left lateral and have consistently lower geodetic slip rate estimates than the current geologic estimate. As there is not a lot of geologic information on the TF fault it may be hard to establish a comparison between the geodetic and geologic rates. Dolan et al. 2007 suggests that the there may be a change in rates based on a partitioning of slip between the San Andreas/Garlock system and the ECSZ. They argue that the seismic cycles and slip along the two systems are anitcorilated (Dolan et et al. 2007). Thus when the Garlock has a period of rapid slip the ECSZ has a period of slow slip. This may explain why we see the Garlock slipping slower than it's geologic rate and why the ECSZ slipping faster than it's geologic rates. However, studies preformed by Malservisi et al. (2003) may suggest that earthquakes cycles affect geodetic surveys. On the other hand, Oskin et al. (2008) point out that at least some portion of the discrepancy cannot be attributed to recent large earthquakes because discrepancies are also present in comparisons using older geodetic measusurements that preceded the earthquakes by several years.

The strain calculations displayed that there are peaks around the western and central portions of the Garlock fault as well as along the Eastern Mojave fault. The maximum shear strain offset along the Garlock could provide evidence for the predominate strain in the area being right lateral. It is possible that strain calculated by geodetic methods could be biased to

postseismic relaxation or a non-uniform strain pulse and not due to a partitioning of strike rat.

Thus the offset in strain may not be supporting Dolan's theory (Oskin and Iriondo 2004; Dawson

et al. 2003).  The dilatational strain displays compressional and extensional regimes that support

clockwise rotation of the Mojave blocks and also supports our block model rotations. Through

this study it has been shown that the strike rate along the Garlock is lower than geologic rates

and has a anomalous right-lateral slip rate to the east. Lower geodetic rates along this fault

system prove that geodetic slip velocities are not always higher than geologic rates.

# References

Cardozo, N., Allmendinger, R.W., SSPX: A program to compute strain from displacement/velocity data. Computers and Geosciences (2008), doi:10.1016/j.cageo.2008.05.008

Chery, Jean. "Geodetic strain across the San Andreas fault reflects elastic plate thickness variations (rather than fault slip rates)." Earth and Planetary Science Letters 269 (2008): 352-65.

Davis, Gregory A., and B. C. Burchfiel. "Garlock Fault: An Intracontinental Transform Structure, Southern California." Geological Society of America Bulletin 84 (1973): 1407-422.

Dixon, Timothy H., E. Norabuena, and L. Hotaling. "Paleoseismology and Global Positioning System: Earthquake-cycle." Geological Society of America 31 (2003): 55-58.

Dolan, James F., D. D. Bowman, and C. G. Sammis. "Long-range and long-term fault interactions in Southern California." Geological Society of America 35 (2007): 855-58.

Frankel, Kurt L., Allen F. Glazner, Eric Kirby, Francis C. Monastero, Michael D. Strane, J. Douglas Walker, Sridhar Anandakrishnan, John M. Bartley, Drew S. Coleman, James F. Dolan, and Robert C. Finkel. "Active tectonics of the eastern California shear zone." Geological Society of America Field Guide 11 (2008): 43-81.

Frankel, Kurt L., James F. Dolan, Robert C. Finkel, Lewis A. Owen, and Jeffrey S. Hoeft. "Spatial variations in slip rate along the Death Valley-Fish Lake Valley." Geophysical Research Letters 34 (2007): 1-6.

Garfunkel, Zvi. "Model for the Late Cenozoic Tectonic History of the Mojave Desert, California, and for Its Relation to Adjacent Regions." Geological Society of America Bulletin 85 (1974): 1931-944.

Malservisi, Rocco, Timothy H. Dixon, Peter C. La Femina, and Kevin P. Furlong. "Holocene slip rate of the Wasatch fault zone, Utah, from geodetic data: Earthquake cycle effects." American Geophysical Union 30 (2003): 1-4.

McClusky, S. C., S. C. Bjornstad, B. H. Hager, R. W. King, B. J. Meade, M. M. Miller, F. C. Monastero, and B. J. B. J. Souter. "Present Day Kinematics of the Eastern California Shear Zone from a Geodetically Constrained Block Model." Geophysical Research Letters 28 (2001): 3369-372.

McGill, Sally F., Stephen G. Wells, Sarah K. Fortner, Heidi A. Kuzma, and John D. McGill. "Slip rate of the western Garlock fault, at Clark Wash,near Lone Tree Canyon, Mojave Desert, California." GSA Bulletin 121 (2009): 536-54.

Oskin, Michael, and Alex Iriondo. "Large-magnitude transient strain accumulation on the Blackwater fault, Eastern California shear zone." Geological Society of America 32 (2004): 313-16.

Oskin, Michael, Lesley Perg, Dylan Blumentritt, Sujoy Mukhopadhyay, and Alexander Iriondo. "Slip rate of the Calico fault: Implications for geologic versus geodetic rate discrepancy in the Eastern California Shear Zone." Journal of Geophysical Research 112 (2007): 1-16.

Oskin, Michael, L. Perg, E. Shelef, M. Strane, E. Gurney, B. Singer, and X. Zhang. "Elevated shear zone loading rate during an earthquake cluster in eastern California." Geological Society of America 36 (2008): 507-10.

Oswald, J. A., and S.G. Wesnousky. "Neotectonics and Quaternary geology of the Hunter

Mountain fault zone and Saline Valley region, southeastern California: Geomorphology." Geomorphology 42 (2002): 255-78.

Peltzer, Gilles, Frederic Crampe, Scott Hensley, and Paul Rosen. "Transient strain accumulation and fault interaction in the Eastern California shear zone." Geological Society of America 29 (2001): 975-78.

Savage, J. C., and R. O. Burford. "Geodetic Determination of Relative Plate Motion in Central California." Journal of Geophysical Research 78 (1973): 832-45.

Savage, J. C., J. L. Svarc, and W. H. Prescott. "Near-field postseismic deformation associated with the 1992 Landeres and 1999 Hector Mine, California, earthquakes." Journal of Geophysical Research 108 (2003): 1-10.

Schermer, E. R., K. A. Stephens, and J. D. Walker. "Paleogeographic and tectonic implications of the geology of the Tiefort Mountains, northern Mojave Desert, California." Geological Society of America Bulletin 13 (2001): 920-38.

Zellmer, John T., Glenn R. Roquemore, and Bruce A. Blackerby. "Modern tectonic cracking near the Garlock fault, California." Geological Society of America Bulletin 96 (1985): 1037-042.